

Process of Converting Ammonia to Hydrogen

Subjects: [Engineering, Mechanical](#) | [Energy & Fuels](#)

Contributor: Yousefi Rizi Hossein Ali , Donghoon Shin

Hydrogen technology for transition to a hydrogen-based economy requires supplying clean and renewable energy and capture of CO₂ from current fossil hydrogen production. Ammonia is the most popular substance as a green hydrogen carrier because it does not carry carbon, and the total hydrogen content of ammonia is higher than other fuels and is thus suitable to convert to hydrogen. Ammonia cracking is a process of producing hydrogen from ammonia decomposition over a catalyst at high temperatures and is preferentially performed at normal pressures.

hydrogen

ammonia

cracking

catalyst

1. Introduction

Hydrogen is a clean fuel and energy carrier playing an important role in a sustainable energy future. When consumed in a fuel cell, the energy content is converted with high efficiency on demand and produces water. Hydrogen can easily integrate into the existing natural gas network with minimal modification but lacks a wide infrastructure, making its storage and transport difficult and expensive ^[1]. Hydrogen technology for transition to a hydrogen-based economy requires supplying clean and renewable energy and capture of CO₂ from current fossil hydrogen production. The ammonia and hydrogen industry has the potential to make significant contributions to global economies with the possibility of using ammonia and hydrogen as fuels ^[2].

2. Process of Converting Ammonia to Hydrogen

Ammonia cracking is a process of producing hydrogen from ammonia decomposition over a catalyst at high temperatures and is preferentially performed at normal pressures. Thermal reactions start at temperatures higher than 773 K without needing a catalyst, while most of the catalytic cracking happens in the presence of a catalyst at temperatures lower than 698 K, with a higher efficiency of about 98–99% ^[3].

The general process flow diagram at scales between 10 kW and 10 MW represents the heat and mass balance of a system (**Figure 1**). The process starts by releasing pure ammonia from liquid storage at a flow rate of 221.5 kg/h (at 500 kW scale) through a feed valve (10–2.5 bar). It is first preheated in heat exchanger (HXpr) by hot output gas of reactor and then its temperature increases to 525 °C with burner combustion (HXref) at a for the reformer. The output gas is then separated under pressure by pressure swing adsorption to produce pure hydrogen and finally discharged at 20 °C ^[3].

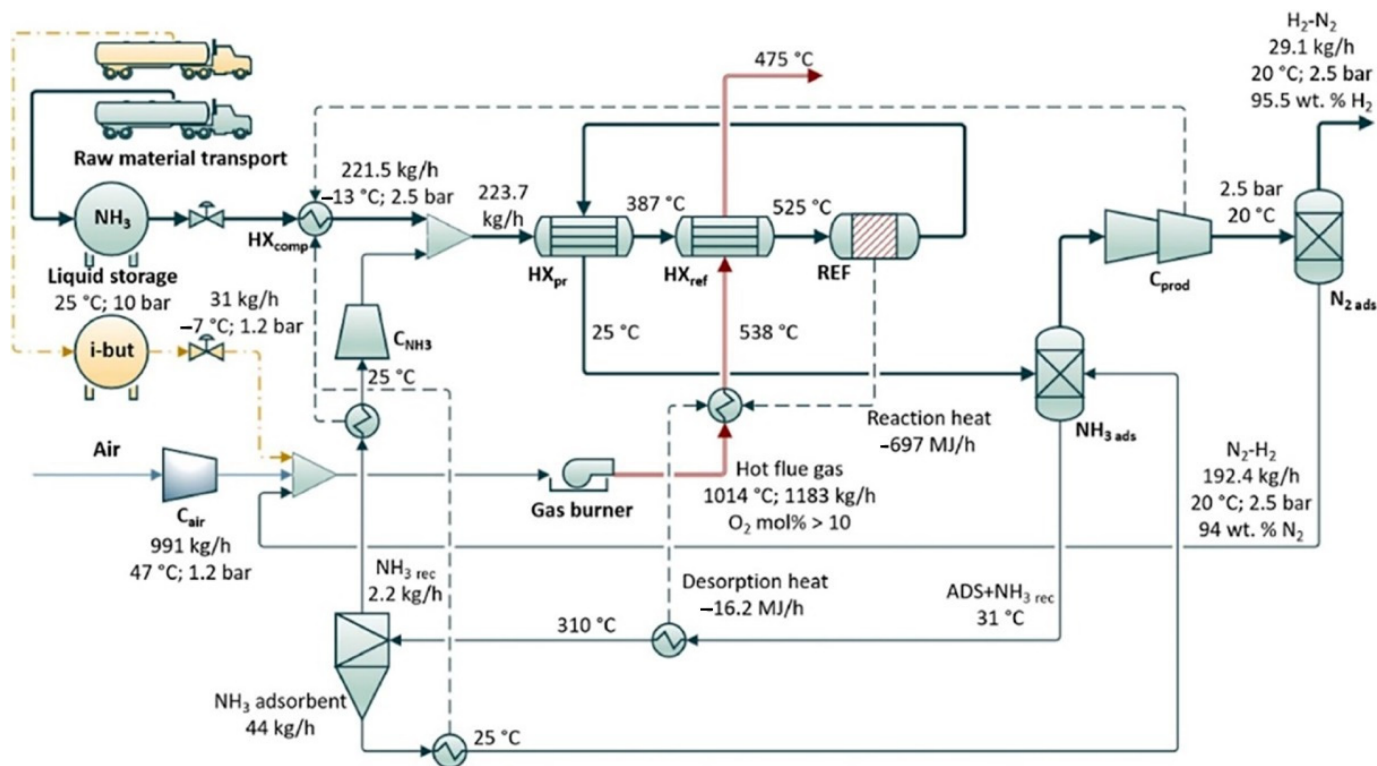


Figure 1. Schematic process flow diagram of the conversion of ammonia to hydrogen and the separation and purification for the simulation model at a 500 kW scale with the output of H₂. Note: HX comp = compressor cooler; HXpr = preheater; HX ref = reformer heat exchanger mantle; REF = reformer; C = compressor; ads = adsorber. Reprinted with permission [3].

2.1. Reactors Technology

Various reactor technologies can be used for the ammonia decomposition reaction, such as microwave, catalytic, plasma, membrane, multistage, continuous tubular, fixed bed, batch and flow bed (Table 1). The catalytic performance of a reactor is related to its type and size, partial pressure, pressure drop, and operating conditions, such as the feed flow rate of ammonia, reaction temperature gradient, and sweep flow rate [4][5][6][7][8][9][10][11][12][13][14][15][16][17][18].

Table 1. Ammonia decomposition reactors, their performance, and their reaction temperatures. Reprinted with permission [5].

Type of Reactor	Properties	Limitation	Performance
Fixed Bed Reactor	High pressure drop; difficulty in maintaining flow rates	Large temperature gradient limits the extent of ammonia decomposition; not suitable for fast catalytic reactions	The higher the feed temperature, the higher the conversion; temperature range 600–900 °C
Microreactor	Characteristic length in the order of sub mm; eliminates	Difficult to scale up for industrial applications; also	Conversion 97.0% with feed of NH ₃ –H ₂ mixture;

Type of Reactor	Properties	Limitation	Performance
	temperature gradient; good for fast catalytic reactions	shows mass transfer limitations in some cases	temperature 400–700 °C; L = 55 mm D = 16 mm; 10 NmL/min P = 1 bar Efficiency = 10.4%
Micropost Reactor	Consists of catalyst-covered pillar-like structures within a microchannel to reduce mass transfer limitation	Conversion depends on pore size; tradeoff required between conversion and pore size; has not been reported yet	Conversion: 85%; flow rate: 15 NmL/min; T = 650 °C P = 1 bar
Fluidized Bed Membrane Reactor	Removal of H ₂ from the reaction zone enhances equilibrium conversion at low temperature; lowers system capital and operating costs	Use of Pd membrane reduces H ₂ selectivity; mostly reported using dilute ammonia; partial pressure of ammonia alters conversion; sweep gas dilutes H ₂	Conversion:(55–99)%, 50–400 NmL/min T = 425–500 °C; P = 1–5 bar;
Catalytic Membrane Reactor	Used-metal-coated sandwich membranes inside catalyst bed	Fixed retentate pressure of 10 bar had to be maintained to ensure sufficient permeation of H ₂	Conversion of 99.93% was attained at a temperature of 550 °C (Conversion: 74.4%;40 NmL/min T = 450 °C; P = 1–3 bar)

In general, in addition to the reactor type, the flow rate of ammonia, partial pressure, dimensions of the reactor, pressure drop, temperature gradient, and sweep gas all play important roles in governing the overall catalyst performance and operating conditions (e.g., reaction temperature, NH₃ feed flow rate and sweep flow rate) [4].

Reactors used in thermal processes require a high-temperature heat exchanger source in addition to the development of catalytic materials [4]. The development of reactor technology for ammonia decomposition can improve reaction kinetics by optimizing the reactor design and relevant conditions in addition to using catalysts to overcome the heat and mass transfer limitations [5]. The differences in conversion can depend on gas flow conditions, deposition methods, and precursor types [19].

2.1.1. Fixed Bed Reactor

Fixed bed reactors, as the most common catalytic reforming reactor for hydrogen production, suffer from poor heat and mass transfer behavior, high temperature gradient, catalyst sintering, coke deposition and dust jamming. The fixed bed reactor enhanced the conversion by increasing the feed temperature to the range of 600–900 °C [7][8][9][10][20][21].

The performance of the fixed-bed reactor for ammonia decomposition was improved using the cobalt-based catalyst, which obtained an ammonia conversion of 87.2% and a hydrogen production rate of 29.2 mmol H₂ gcat⁻¹ min⁻¹ at 500 °C with a space velocity of 30,000 mL gcat⁻¹ h⁻¹ [11]. Furthermore, the ammonia conversion over a Ru-based catalyst (with different Cs) (**Figure 2**) was improved by increasing the Cs/Ru molar ratio up to 4.5 at lower temperatures of 325 °C but did not increase over a Ni-based catalyst in a fixed-bed reactor at 800 °C [12][22].

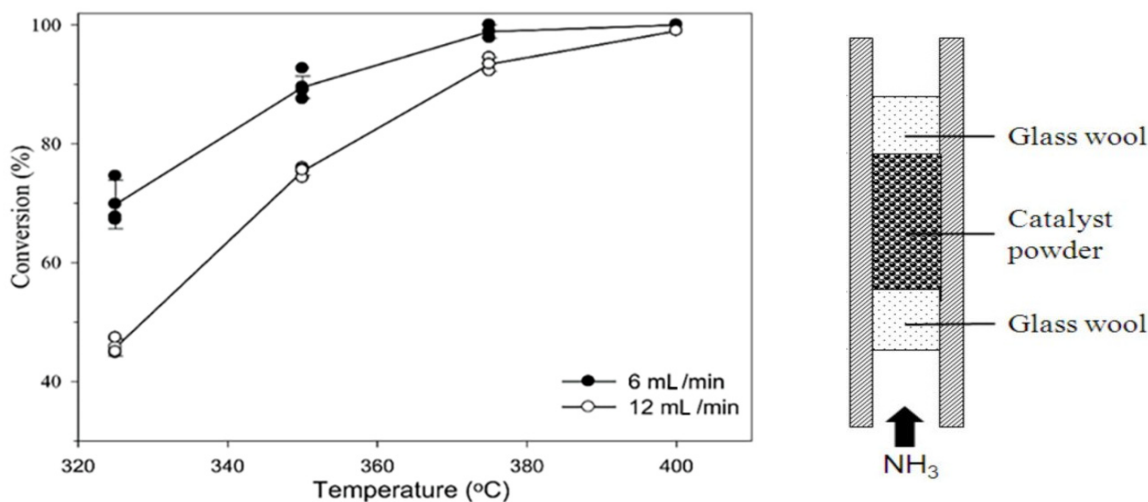


Figure 2. Ammonia decomposition with the tubular fixed-bed reactor and Cs/Ru catalyst. Reprinted with permission [12][23].

Various types of catalytic reforming reactors can be used based on their properties and their performances. The different types of reactor technologies with inter-stage heating and some differential elements can be found in [8][10][14]. The optimization of reactor parameters with a pure phase of $\text{Ni}_2\text{Mo}_3\text{N}$ catalyst using a chelating method of preparation for high catalytic activity resulted in an ammonia conversion rate of 97% at 525 °C [12]. A schematic diagram of the preparation of hollow fiber reactors, the deposition of Ru-NCX on the Al_2O_3 substrate through sol-gel, and pyrolysis and Ru incipient wetness impregnation methods is displayed in Figure 3 [24]. The on-board hydrogen production technology uses hollow fiber converters (HFC) in compact ammonia cracking reactors due to the advantage of minimizing the weight and space of the catalyst (smaller volume of 93%, catalyst loading of 80%) while enhancing ammonia decomposition efficiency compared to general packed bed reactors (PBR). The HFC reactor represents a uniform distribution of the catalyst on the substrate and is cheaper than the PBR (Figure 4). The HFC is cheaper because it uses less precious metal-based catalyst (80 wt%). It is more efficient in mass transfer, has lower pressure drops of 99%. It can improve the residence time distribution, and improves the reaction kinetics (internal and external diffusion limitations), which results in a larger conversion rate (4 times at 773 K) than PBR. Therefore, it has the potential for economical production [24].

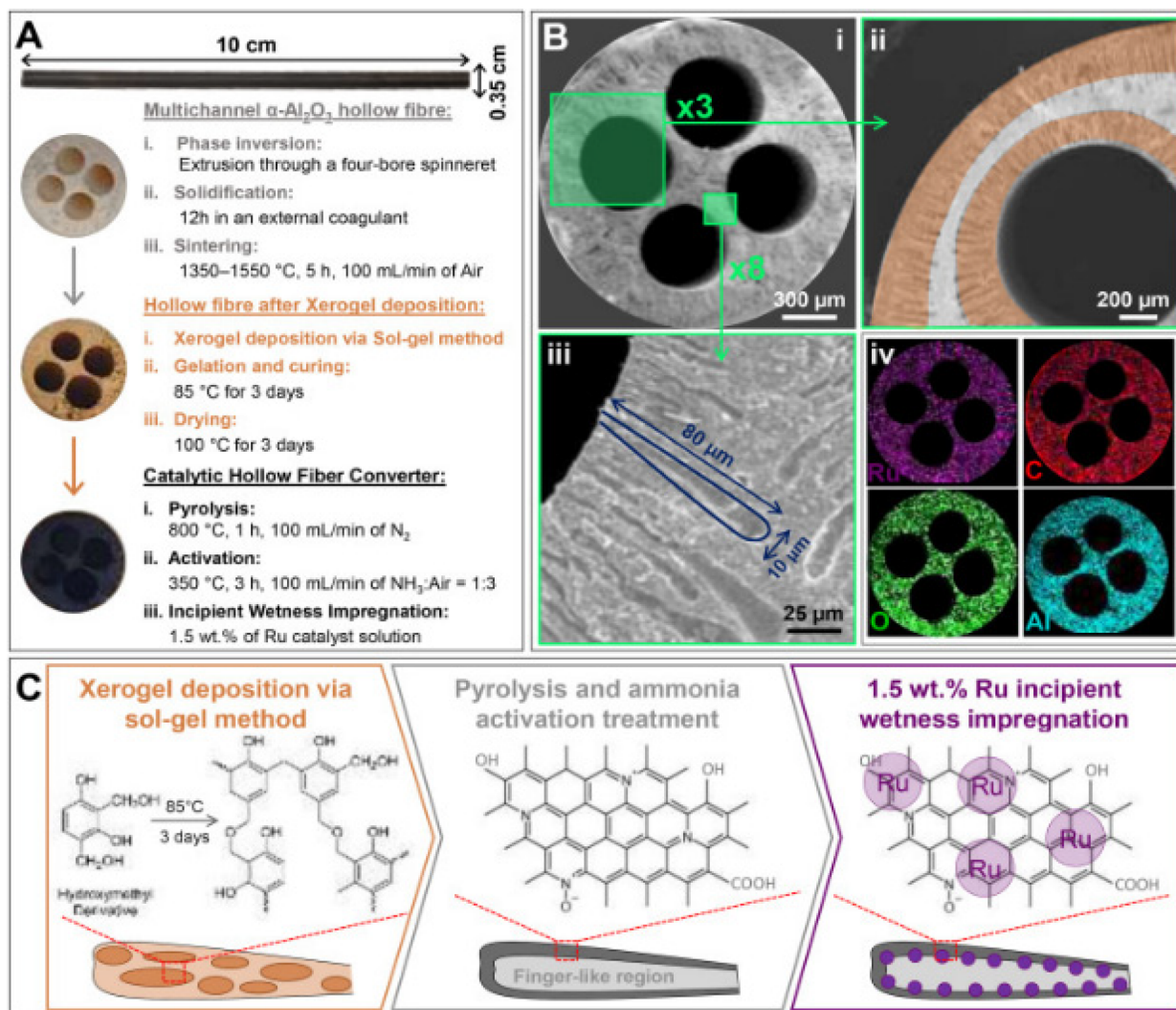


Figure 3. (A) the morphology of the hollow fiber, after the sol-gel impregnation with the precursor xerogel solution (B) SEM images of the cross-section of the 4-channelled hollow fiber, at different magnifications (i–iv), and the use of a precursor liquid solution results in the catalyst being uniformly dispersed. (C) deposition layers of the Al_2O_3 hollow fiber with the Ru-NCX catalyst in three steps of polymerization, carbonization and incipient wetness impregnation. Reprinted with permission [24].

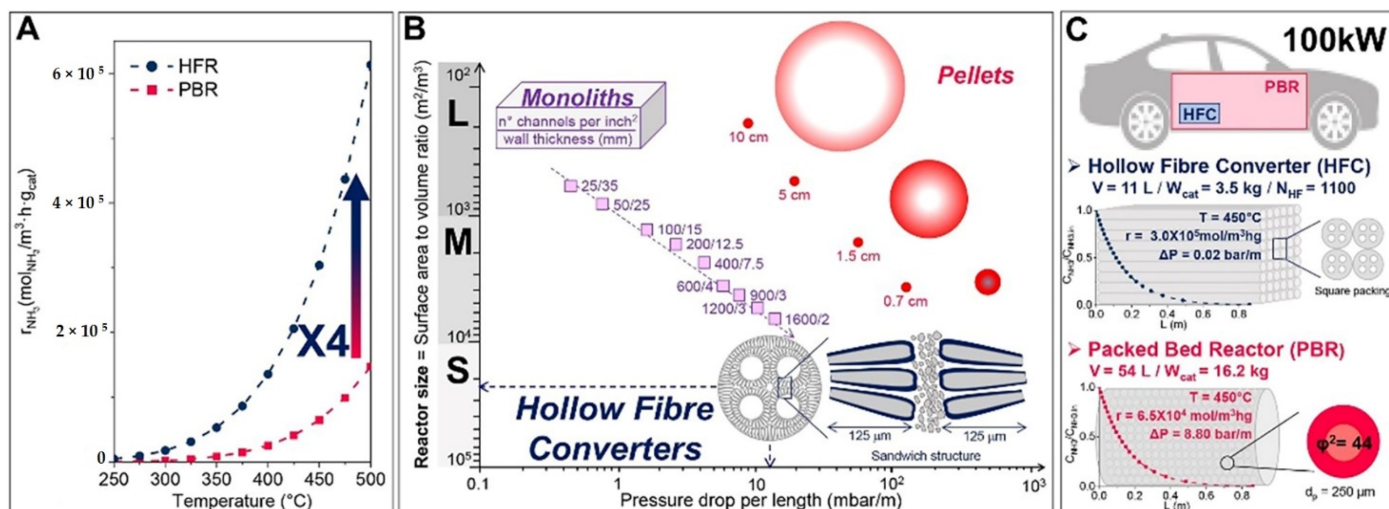


Figure 4. (A) Compression of the fixed bed PBR and the HFR decomposition rate by temperature, (B) the size of reactors and their pressure drop per length, (C) designed reactor for 72 m³/h H₂ supply of a 100 kW car. Reprinted with permission [24].

2.1.2. Fluidized Bed Reactor

A fluidized bed shows its advantage in the industrial-scale catalytic reforming process because the surface of catalysts could be separated continuously. The features such as the sweep gas effect, bubble-to-emulsion mass transfer, densified zone formation and concentration polarization are impacted by the fluidized bed membrane reactor [20][24][25][26][27]. Moreover, the membrane-assisted fluidized bed reactor has good gas–solid contact and heat and mass transfer characteristics, which can increase catalytic reforming and improve hydrogen production [7][8][9][10][20][21].

However, conventional Pd-based fluidized bed membrane reactors (FBMR) are not suitable for ammonia decomposition due to their low performance, under the same operating conditions. Also due to weight, volume, and start-up time, they are not applicable for PEM fuel cells in on-board hydrogen production [5][8][9][10][14][20][21].

2.1.3. Membrane Reactor

Membrane reactor technology with a high conversion rate can be used for ammonia decomposition with a high hydrogen flux. It is prepared by coating the porous supports and protective layers, such as a porous ceramic tube with a Ni/La-Al₂O₃ catalyst or a hydrogen-selective silica membrane deposited on porous tubular alumina Ru/γ-Al₂O₃/α-Al₂O₃ bimodal catalytic support. (Figure 5)[13][16]. A palladium membrane reactor (PMR) supported by porous stainless steel with a Na/Ru-carbon catalyst can be used for ammonia decomposition due to its kinetically enhancing effect [14][28]. The hydrogen separated and generated with a high-purity simultaneously within the same unit [8][13][14][15][16]. The ammonia conversion can increase the thermodynamic equilibrium and kinetic enhancement effect of hydrogen removal through the membrane walls. High hydrogen separation efficiency can be achieved at

lower temperatures compared to conventional systems. Using a membrane reactor combined with a solar heat absorption system can lead to energy and economic benefits [7][8][13].

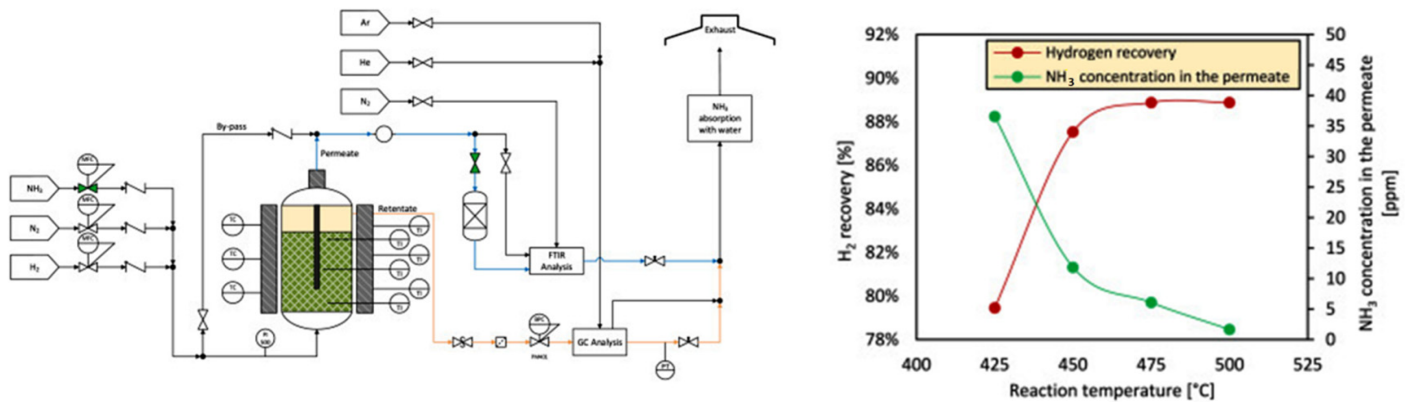


Figure 5. The effect of reaction temperature of the ammonia decomposition over a Pd-based membrane (PMR) on hydrogen recovery and ammonia concentration in the hydrogen permeate. Reprinted with permission [13][16].

The membrane reactor recovers the hydrogen of ammonia decomposition and simultaneously separates it with high purity at lower temperatures and lower costs compared to conventional systems. **Table 2** and **Table 3** demonstrate the performance of hydrogen recovery and the permeation through the Pd membrane at different temperatures for the Cs/Ru catalytic membrane reactor [15][16].

Table 2. Hydrogen permeating through Pd membrane before and after ammonia decomposing at different temperatures. Reprinted with permission [29].

Permeation (mol cm ⁻² s ⁻¹ pa ⁻¹)	350 (°C)	400 (°C)	450 (°C)
Before			
H ₂	4.19 × 10 ⁻¹¹	5.52 × 10 ⁻¹¹	6.46 × 10 ⁻¹¹
N ₂	Not measurable at 5 × 10 ⁵ pa		
After			
H ₂	6.64 × 10 ⁻¹¹	8.25 × 10 ⁻¹¹	9.91 × 10 ⁻¹¹
N ₂	4.42 × 10 ⁻¹⁴	N/A	N/A

Table 3. Comparison of the performance of catalytic membrane reactor with the packed bed membrane reactor. Reprinted with permission [29].

Specifications of Reactor	CMR	CMR	PBMR
Temperature (°C)	400	450	520
Pressure (Mpa)	0.5	0.5	0.3
Ammonia flow rate (cm ³ /min)	61.3	207.3	150
Conversion (%)	98	95.7	98
Purity (%)	98.7	99.7	99.2
Recovery (%)	85.7	78.6	66
Productivity (mol m ⁻³ s ⁻¹)	8.1	23.9	3.6
Ru loadings (mgRu/cm ²)	1.43	1.43	11.68

The performance of a conventional reactor can be enhanced by adding a membrane system, which leads to achieving a conversion beyond the thermodynamic restrictions. At temperatures above 425 °C, the ammonia conversion was higher than 86%, and the hydrogen purity was 99.998%. The application of a vacuum to the permeable side of the membrane leads to higher hydrogen recovery and enhanced ammonia conversion in compare with thermodynamic equilibrium conversion. Furthermore, the ammonia conversion was not majorly changed by the reactor feed flow rate and operating pressure [13].

The various types of membranes, such as microporous ceramic, crystalline and amorphous, dense metal and proton conducting, perovskite and non-perovskite, are displayed in **Figure 6** [8][30]. The influencing factors of membrane separation are including membrane material, membrane sealing, membrane pollution, carbon monoxide poisoning, and membrane arrangement [18]. In the case of dense metallic membranes, hydrogen adsorbed at the surface dissociates into two hydrogen atoms that can diffuse through the metal lattice [18].

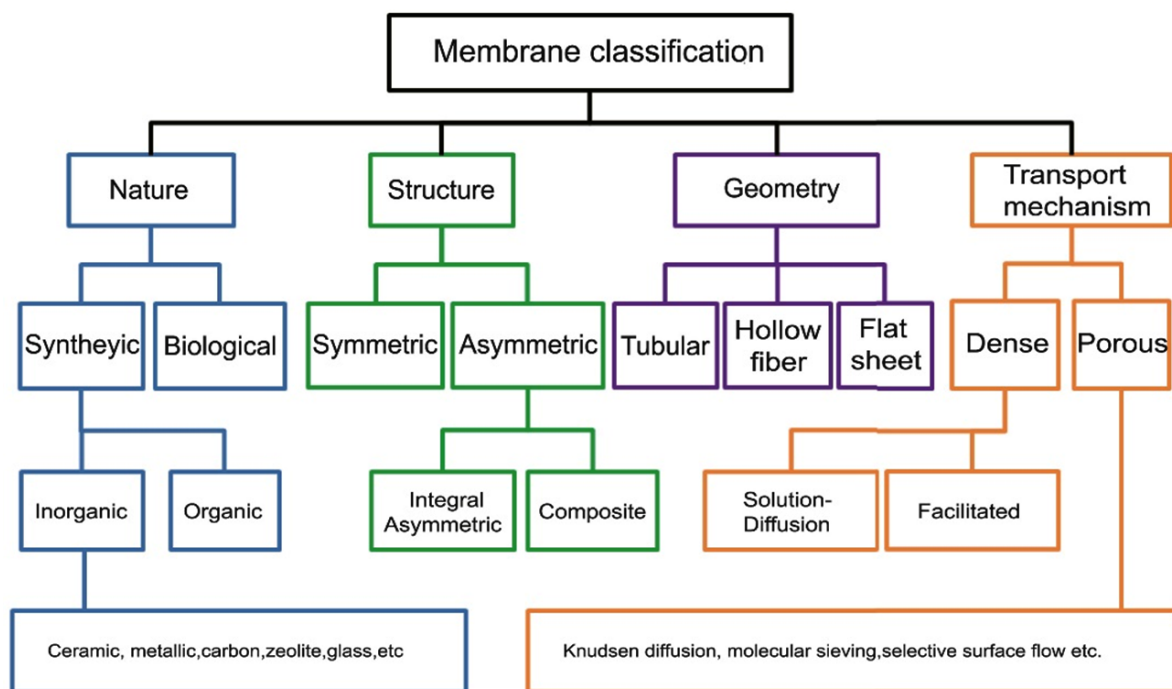
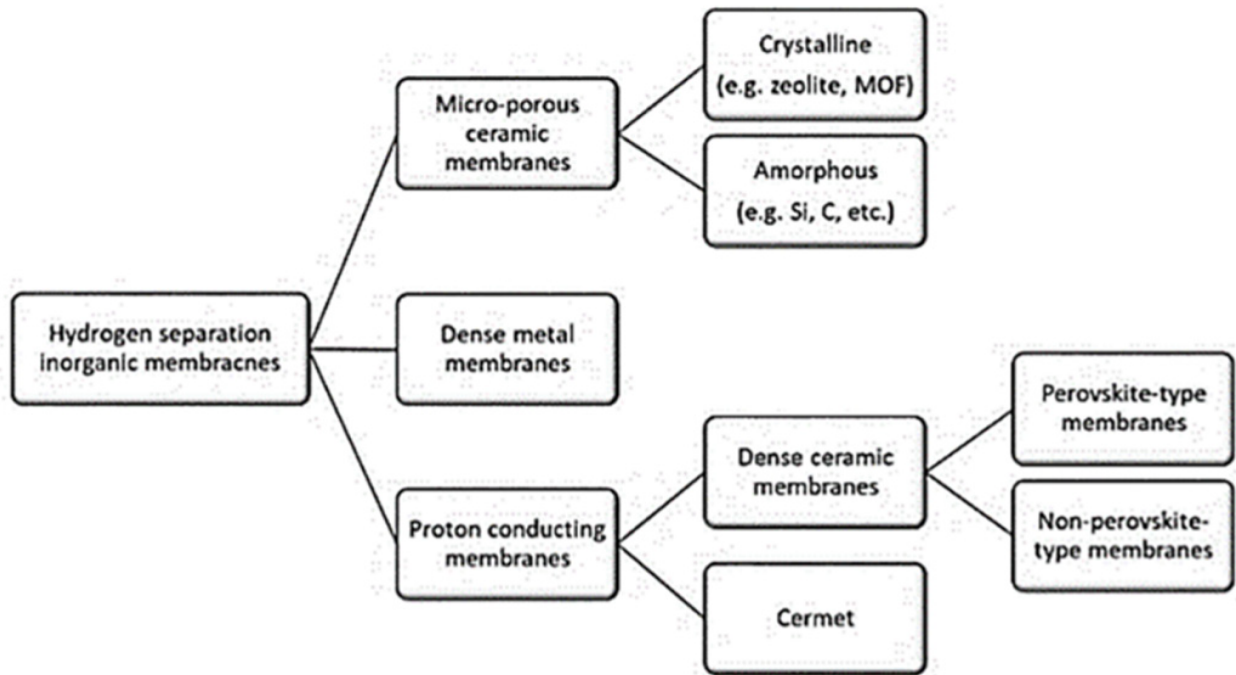


Figure 6. Classification of membranes (a) Membrane reactors based on their different properties (b) Variety of membrane classes. Concerning their mechanism, depending on specific properties of the components, molecules/membrane surface interactions (e.g. multi-layer diffusion) and/or difference between the average pore diameter and the average free path of fluid molecules (e.g. Knudsen mechanism); the difference of diffusivity and solubility of substances in the membrane, the difference in charge of the species to be separated: electrochemical effect. . Reprinted with permission [8][31].

2.1.4. Other Types of Reactors

The solid oxide fuel cell (SOFC) directly generates electricity efficiently through hydrogen produced from ammonia at temperatures between 500 and 800 °C with low energy efficiency (Figure 7)^[25]. Therefore, it is requiring to development of catalysts, for improving conversion rates at low temperatures ^{[25][26]}.

Microfabricated reactors and some monolithic reactors were used for the decomposition of ammonia with a flow rate of 500 NmL/min over a spherical Ni–Pt/Al₂O₃ catalyst at atmospheric pressure, in portable fuel cell power supply. High hydrogen conversion (>99%) and operability were reached at a temperature of 873 K, but their energy efficiencies were low (<15%). The porosity and permeability of the packed bed are not parameters of engineering importance, and hence, they did not significantly affect the performance of the reactor ^{[8][27]}. There was comparison of microreactors characteristics between the micropost (conversion of 85%, flow rate of 15 NmL/min, and temperature of 650 °C); with the microreactor (conversion of 97.0%, flow rate of 10 NmL/min feed of NH₃–H₂ mixture, temperature of 400–700 °C) ^[12].

The microwave reactor has a high conversion at lower reaction temperature due to its selective heating properties, which can directly transfer the energy required for the ammonia decomposition reaction from the microwave systems to the active surface; however, the formation of a hot zone and heat losses are problems that need to be solved ^[32].

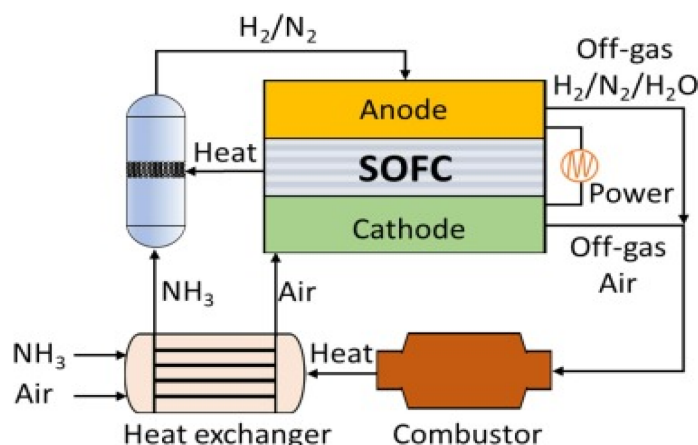


Figure 7. Schematic reactor integrated with SOFCs with combined heat, power and rate of ammonia decomposition^[25].

2.2. Catalysts for Ammonia Cracking

Ammonia decomposes with adsorption over the catalyst surface and releases hydrogen in a stepwise sequence reaction. High ammonia conversion is possible at lower temperatures thermodynamically, but yet higher reaction temperatures are required (due to kinetic limitations), as well as the presence of an active catalyst. In this regard, different catalysts, promoters and support materials can be used for the required industrial application. Besides these, the supports metals and binding energy can be controlled for catalyst efficiency and suitability. The development of catalysts for economic and high-performance decomposition depends on their activity, long-term thermal stability, lifetime, lower pressure drop and system integration ^{[3][27]}.

2.2.1. Catalysts Characterization, Activity and Performance

Catalytic ammonia cracking is a general technology for producing hydrogen. These catalysts consist of a transition metal, a promoter, supporter, and/or a second catalytic metal. The several factors need to be considered in the assessing of different catalysts, such as, pure metal catalysts, oxides or alloys, cost, long-term stability, and efficiency. This could include noble or precious metals and non-precious metals based on their costs, types and properties [26][33].

The most precious metals used as catalysts in catalytic decomposition include Cr, Co, Cu, Fe, Ir, Ni, Pd, Pt, Rh, Ru, Se, and Te, alloys of aluminum oxide with nickel, Ru and Pt, and alloys of iron with other metal oxides, and examples of non-precious metals include Al, Ce, Si, Sr, and Zr [33][34][35][36].

Catalysts can also be categorized into perovskite and non-perovskite types based on the similarity of their crystal structures to mineral calcium titanium oxide (CaTiO_3). There is a subgroup of perovskites that consists of heavier halides (Cl, Br, and I), both fully inorganic and hybrid organic–inorganic ones, as well as the many variants. They exhibit unique sensitivity and long-term stability. Moreover, catalysts with metal–support interaction enhancement, the application of promoters, and bimetallic alloys have also been developed to overcome the high activation energy barrier [12][37][38].

Catalyst reaction rates and catalytic activity can be enhanced by the type of active metal, type of support material with good physical properties, particle size, surface area, dispersion of the catalyst, and activity of the promoting material. The presence of the additives and the alteration of the support material can modify the nitrogen desorption step and the catalytic properties of the catalyst, such as Al_2O_3 – TiO_2 , which is used commercially as a support for the catalysts [39][40].

The catalytic activity and performance of different single-metal catalysts are in the order of $\text{Ru} > \text{Ni} > \text{Rh} > \text{Co} > \text{Ir} > \text{Pt} \cong \text{Fe} > \text{Cr} > \text{Pd} > \text{Se} \cong \text{Cu} > \text{Te} > \text{Pb}$, respectively [10]. Various high activity elements can be used as catalyst supports to replace the expensive Ru for the economical cracking of ammonia to hydrogen [41]. The catalytic activity varies with different ammonia concentrations and different types of support materials, such as platinum or palladium, or for example, for Ni components, i.e., $\text{Ni}/\text{Y}_2\text{O}_3 > \text{Ni}/\text{Gd}_2\text{O}_3 > \text{Ni}/\text{Sm}_2\text{O}_3 > \text{Ni}/\text{La}_2\text{O}_3 > \text{Ni}/\text{Al}_2\text{O}_3 > \text{Ni}/\text{CeO}_2$ [41][42].

The performance of catalysts can be evaluated by the turnover frequency (TOF) as a quantifying rate of reaction in terms of catalytic activity and decomposition conditions. The TOF is the number of moles of reactant consumed or moles of product per mole of catalyst per unit of time (s^{-1} or h^{-1}), which is significantly influenced by the catalytic activity of different catalysts metals [27][42], the catalysts nitrogen adsorption energy [38], and particle size [43]. The catalytic activity is generally lowered with a reduction in the catalyst particle size, for example, in nickel-based catalysts [43]. It is also influenced by the forms (pelletized and powder) of the supported materials [3].

Moreover, the activity for single-metal catalysts, is a function of the nitrogen binding energies ($Q_{\text{N}(0)}$) [33]. The TOF is defined in terms of turnover number (TON) and time of reaction, as in the following equation [42][44]:

$$\text{TOF} = \frac{\text{TON}}{\text{time of reaction}} \quad (1)$$

where the turnover number (TON) is a dimensionless value, defined as the number of moles of reactant consumed per mole of catalyst before deactivation under given reaction conditions [19]. The TON is an important parameter for evaluating the stability of the catalyst and is associated with the temperature, the concentration of the substrate, the deactivation of the catalyst and its pre-activation (zero slope), as shown in **Figure 8**[45]. The decomposition conditions significantly influence their catalytic performance and can provide a real measure of the efficiency of a catalyst [40][41][42][44].

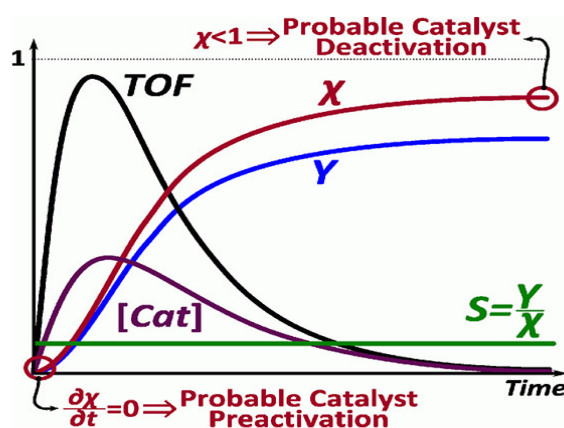


Figure 8. Model of active catalyst concentration and the turnover frequency (TOF). Reprinted with permission [46].

Nanocarbon technology can contribute to the commercialization of hydrogen production from ammonia by increasing the catalyst performance, reaction surface area, reactivity, secured durability and expanding facilities. The catalytic ability of nanostructured electro-catalysts usually varies with size and morphology [47].

2.2.2. Ru-Based Catalysts

Ru is the most active metal among Ru, Rh, Pt, Pd, Ni, and Fe supported on carbon-based supports and metal oxides. Theoretical studies support the fact that an Ru surface has optimal binding energy with a nitrogen atom, leading to the highest ammonia decomposition activity among mono-metals (**Figure 9**) [7][37][38][25][48][49]. An Ru-based catalyst for ammonia conversion has the highest turnover frequencies (TOF) among the single-metal catalysts, which is presented as a function of the nitrogen binding energies ($Q_{N(0)}$ kcal/mol), as shown in **Figure 10**[50].

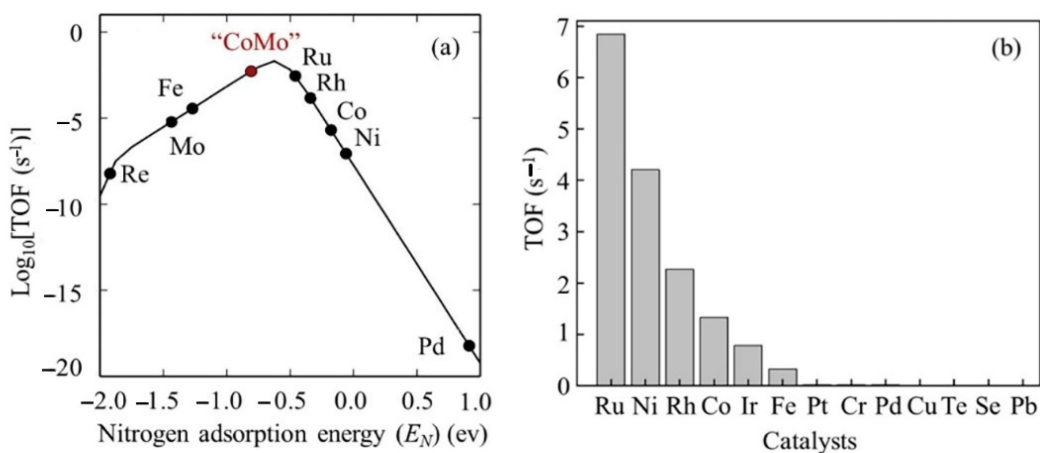


Figure 9. Turnover frequency (TOF) (a) as a function of nitrogen adsorption energy and (b) various precious metal catalysts. The red point "CoMo" indicated the mixed of both Co and Mo metal catalysts. Reprinted with permission [3].

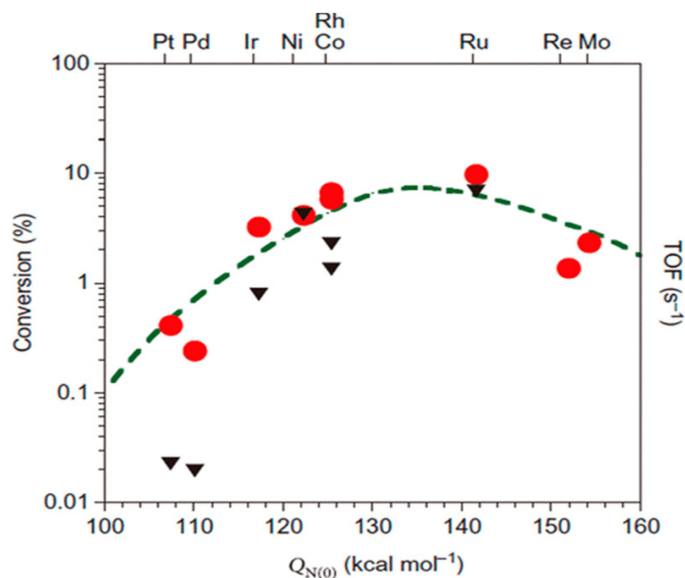


Figure 10. Comparison of turnover frequencies (TOFs) of supported catalyst for ammonia decomposition by modeling (circles, left axis) and experimenting (triangles, right axis) at 850 K. Reprinted with permission [50].

Ru-based catalysts supported on carbon materials (Figure 11) have been proposed as the most efficient catalysts for the ammonia cracking reaction [33][34][35][36]. Using Ru or Cs-Ru as a catalyst, carbon powder pre-treatment solutions and catalyst deposition conditions were obtained with a maximum ammonia conversion rate of 90% and hydrogen generation rate of $29.8 \text{ mmol/min } g_{\text{cat}}$ at 673 K. Ru, when supported on carbon nanotubes (CNTs), increases decomposition conversion, achieving an ammonia conversion level of about 84.65%, with an H_2 formation rate of $28.35 \text{ mmol/min } g_{\text{cat}}$ and maintaining the effective area of the catalyst under reaction conditions, ambient pressure and a temperature of 773 K. This is due to the high dispersion of Ru particles and the inhibition of particle growth of the catalyst, resulting in the stability of the catalyst and high catalytic activity [33][34][35][36]. The performance of the catalysts for the ammonia decomposition reaction can be enhanced by applying them over

different supported materials, such as ruthenium-based catalysts on carbon materials, as the most suitable supports include active carbons, high surface area graphite carbon CNTs, and carbon nanofibers [51][52][53].

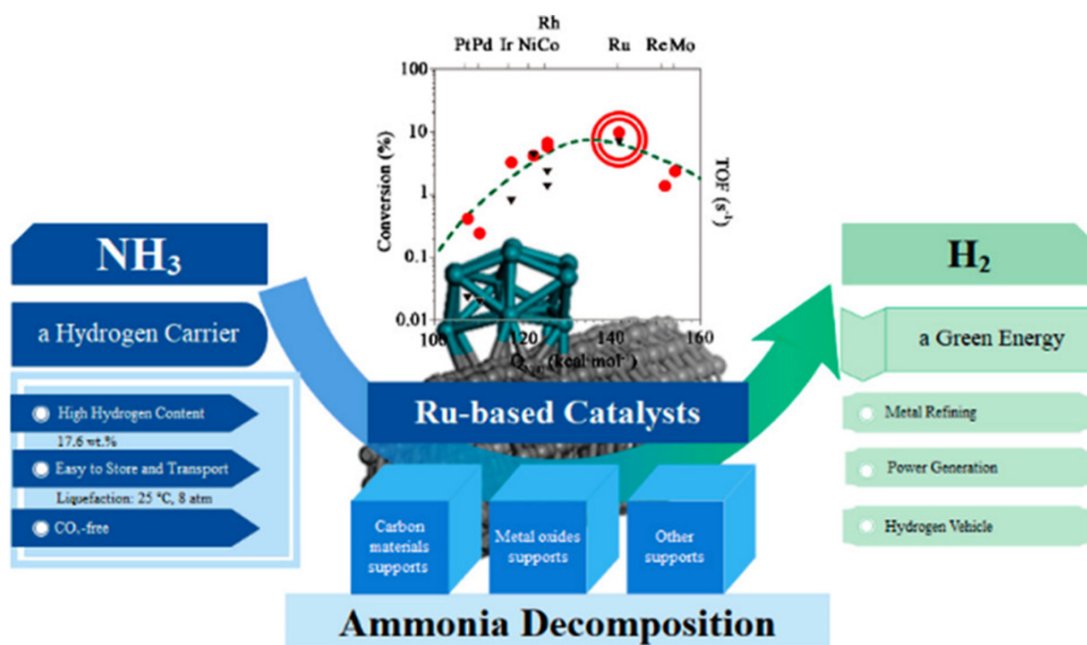


Figure 11. Ru-based catalysts for ammonia decomposition. Reprinted with permission [33].

Due to the properties of an Ru-NCX heterogeneous hybrid nanocomposite catalyst containing Ru, N, and C atoms, the activity and durability of the release of hydrogen from ammonia at temperatures ranging from 475 to 550 °C were enhanced compared to Ru. If the Ru catalyst was fixed through the activation process using the CO₂ of a carbon xerogel (Figure 12), the decomposition rate was 3.5 times higher than that of the existing deactivated catalyst at 450 °C. Carbon support, nitrogen, and sodium elements were used to promote the activation of the catalyst [24][47][51].

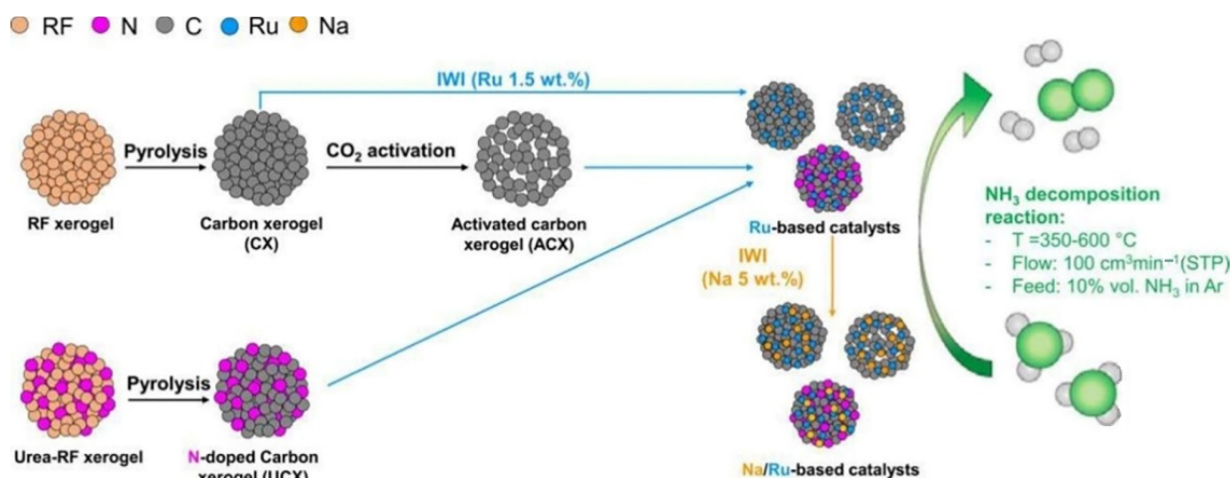


Figure 12. Development process of resorcinol–formaldehyde carbon xerogel for Ru-based catalyst. Reprinted with permission [51].

Some Ru-based catalysts are used for ammonia cracking, such as Ru/CNTs, which have higher catalytic activity than Ru/MgO, Ru/AC, Ru/ZrO₂, and Ru/Al₂O₃ respectively (**Table 4**). In addition, adding a potassium (K) promoter increased the ammonia conversion to about 97.3% and resulted in a hydrogen formation rate of 32.6 mmol/(g_{cat} min) at an ammonia flow rate GHSV of 60,000 mL/(g_{cat} h) at 450 °C [33]. After the Ru/CNT was modified with potassium nitrate, carbonate or potassium hydroxide (KOH) as the best promoter, the rate of ammonia cracking and the rate of hydrogen evolution significantly improved to 99.74%, and the hydrogen formation rate reached 47.88 mmol/min g_{cat}. The Ru-based catalysts (Ru-Na/CNT) have shown a high conversion of ammonia (100%) at a low temperature of 673 K. The high activity of ruthenium nanoparticles was with sizes in the range of 3 to 5 nm [43].

Table 4. Summary of ammonia decomposition catalysts based on reaction temperature, performance, conversion and efficiency rates. Reprinted with permission [33].

Catalyst/Support	Temp. (K)	Conv. Eff. Rates (%)
Ru/Al ₂ O ₃ at (1 bar)	673	99.00%
Ru/Al ₂ O ₃ at (5 bar)	673	96.00%
Ru/Al ₂ O ₃ at (5 bar)	773	99.00%
Ru/Al ₂ O ₃ at (10 bar)	673	92.00%
Ru/Al ₂ O ₃ at (10 bar)	723	95.50%
Ru/Al ₂ O ₃ at (10 bar)	773	97.20%
Ru/La–Al ₂ O ₃ pellet catalyst	773	99.7%
Ru/CNT treated with KOH	773	99.74%
Ru, when supported on carbon nanotubes (CNTs),	773	84.65% with an H ₂ 28.35 mmol/min g _{cat}
Ru or Cs-Ru, carbon powder pre-treatment solutions and catalyst deposition conditions	673	90%, H ₂ 29.8 mmol/min g _{cat}
Ni components		
Ni/Al ₂ O ₃	823	98.30%
Ni-CeO ₂ /Al ₂ O ₃	873	99.90%
Ni/SBA-15	873	96.00%
Ni well-dispersed layers on mesoporous γ-Al ₂ O ₃	880	98%
Na/NaNH ₂	800	99.20%
CsH ₂ PO ₄	796	96% for 1.48 mol H ₂ /g _{cat} h

Catalyst/Support	Temp. (K)	Conv. Eff. Rates (%)
Fe–MOx Ce, Al, Si, Sr, and Zr		
N/Fe/TiO ₂ (NFT)	298	60% with radiation
CuO on TiO ₂ nanotube rows (TiNTAs)	298	50.1% with radiation
Rb precursor in Al-anodized Al ₂ O ₃ micro-reactor	873	converts 99% into the equivalent of 60 W of hydrogen
Nitride and carbide catalysts Carbides and nitrides of Fe, Co, Ni, Ti, V, Mn, and Cr	623–923	96–98%
Metal amides/imides, alkali metal amides as sodium amide (NaNH ₂), lithium amide, Li ₂ NH.	Below 723 above 873	99%
Bimetallic catalysts, molybdenum, cobalt, CoMo and traces of Co added to Fe, PtSn/Mgo, Pd, Cu, Ge	below 600 K	96%

different cesium (Cs) loading at lower temperatures of 325–400 °C in the fixed-bed reactor showed the Cs effects on the ammonia conversion at a higher Cs/Ru molar ratio. Enhancing the Cs/Ru molar ratio increased the ammonia conversion with a maximum value of 4.5 as the optimum Cs loading, with almost 100% of the ammonia converted (with the GHSV (gas hourly space velocity) from 48,257 to 241,287 mL/(h·g_{cat}), at 400 °C [12].

According to **Figure 13**, the ammonia decomposition conversion increased over the Ru (2 wt%)/La (20 mL%)-Al₂O₃ at temperatures of 350 to 550 °C under different GHSVs of 5000–30,000 mL/gcat hr and catalyst loadings. The TOF comparisons of various Ru supported on pelletized and powder forms show, among powder forms, that KCNTs have the highest and TiO₂ has the lowest, and in pelletized forms, La Al₂O₃ has the highest value of TOF [3].

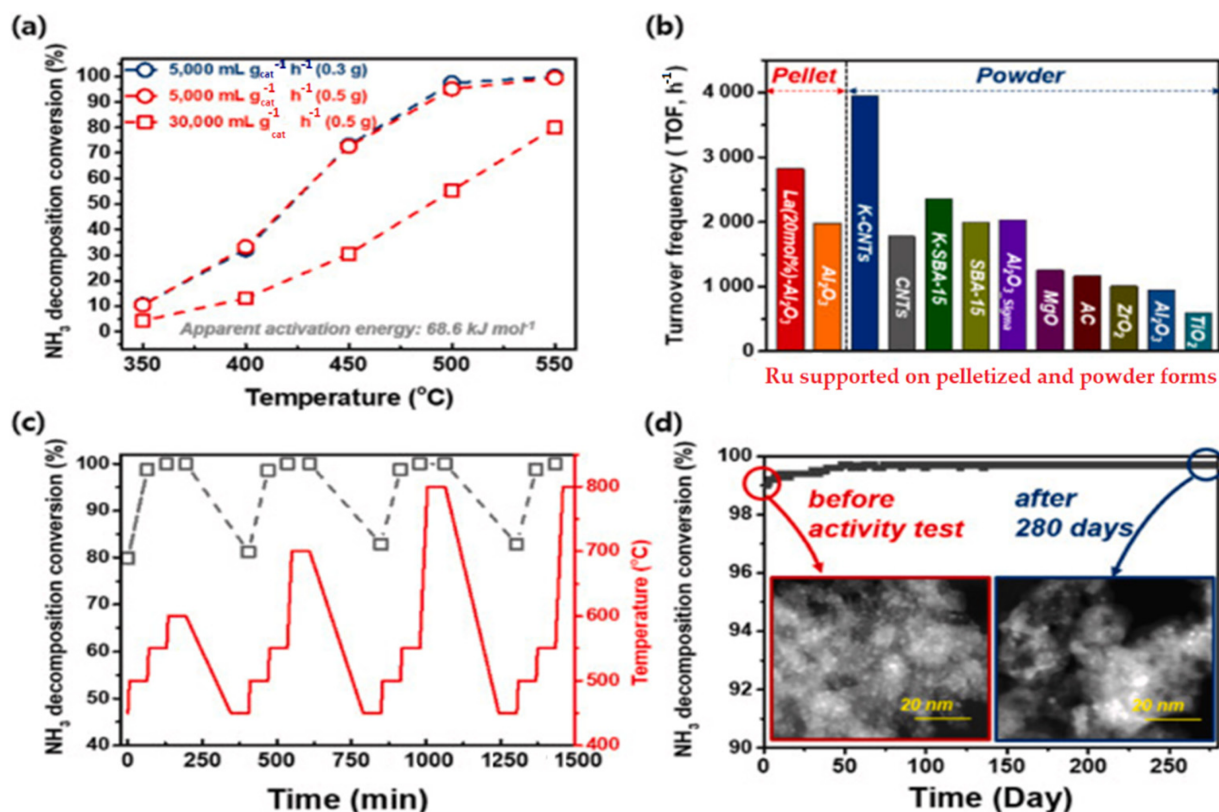


Figure 13. Catalytic activities of Ru/La Al₂O₃ under different GHSVs with varying catalyst loadings (a); TOF comparisons of various Ru supported on pelletized and powder forms (b); catalytic activities with varying temperatures (c); TEM images of durability tests of the catalyst over 280 days (6700 h) (d). Reprinted with permission [3].

The perovskite catalyst Ru/La–Al₂O₃ pellet had a high catalytic activity of 2827 h⁻¹ at 450 °C and stability for over 6700 h at 550 °C, exceeding the performance efficiency of 83.6% for producing hydrogen over 66 L/min. According to **Figure 13**, the simulation of the typical ammonia hydrogen production process showed that the performance of the pellets with the Ru(2 wt%)/La–Al₂O₃ perovskite structure is 98% or higher at 550 °C [3].

Although Ru-based catalysts show the highest catalytic activity in high ammonia concentrations at the temperature of 425 to 500 °C, it has the disadvantage of scarcity and quick deactivation that impedes the large-scale application of ammonia decomposition, and it is expensive, resulting in a high cost of ammonia decomposition [11].

2.2.3. Non-Ru-Based Catalysts

Ammonia hydrogen production technology has a clear tendency to replace expensive Ru-based catalysts with other materials [3]. High catalytic activity of the non-Ru catalysts can be achieved by modifying the primary catalyst component, adding promoter and support materials, and using inactive metals with further treatments of surface modifications and alloying techniques [40][54]. Ammonia decomposition at low temperatures with advanced catalyst that are cheaper than ruthenium, need to consider the mechanisms of the reaction kinetics, the effects of catalyst

formulation and synthesis, catalyst modification including promoters and supports, and increasing the efficiency with nanotechnology and using two or more promoters at the same time [5].

Various types of transition metals, including promoters and supports, have been developed to replace precious catalysts. It is important to develop transition metal catalysts with low cost and high stability, such as Fe, Co, and Ni, etc. Among them, cobalt has been considered a replaceable metal of Ru due to its low cost and nitrogen adsorption [11].

Polycrystalline foils and wires made of Pd and Ir were used at low temperatures from 500 to 1190 K to reduce the mass of the catalyst, demonstrating the impact of catalyst form on the performance of ammonia decomposition and showing an improvement in the reaction rate. The decomposition rate of ammonia on Ir was high compared with other metals (Ir > Rh > Pt > Pd), respectively [27].

Ammonia decomposition over a series of fine powders of a Fe–MO_x catalyst (M represents different metal components Ce, Al, Si, Sr, and Zr) showed that Fe–(Ce, Zr)O₂ was highest because the additive (Ce, Zr)O₂ solution worked as a solid acid to enhance the ammonia adsorption and reaction probability of Fe components at relatively low temperatures. A CeO₂ promotor was used to increase the catalytic activity by the surface area of the catalyst, and Ni/Al₂O₃ was used for the stability of catalysts for ammonia decomposition, resulting in a conversion of 98.3% and hydrogen formation rate of 32.9 mmol/min g_{cat} at 823 K [33][34][35][36].

One example of an alternative catalyst includes layers of well-dispersed Ni on mesoporous γ -alumina. This catalyst is low cost, stable and exhibits high activity, achieving complete conversion of pure NH₃ at a temperature of 880 K, which makes this catalyst a promising candidate for in-situ H₂ generation from ammonia to feed fuel cells in vehicles or industry [33][34][35][36].

The decomposition rate increases with the partial pressure of ammonia on surface sites of the basal planes of metals such as tungsten, platinum, and molybdenum sulfide (MoS_{1.65}) nanocrystals at high temperatures [5][55]. The activity of ammonia decomposition improves by combining bimetallic catalysts, such as molybdenum, which has a high nitrogen binding energy with cobalt with a low binding energy and adding traces of Co to Fe [5].

Metal-sulfide photocatalysts are used in hydrogen production, CO₂ reduction, pollutant decomposition, and N₂ fixation due to their suitable band-gap energy, active sites, and outstanding optoelectronic properties [27]. Other alternative catalysts to expensive metals are nitrides and carbides of transitional metals, such as Fe, Co, Ni, Ti, V, Mn, and Cr, which have a high activity, as their N₂ nitrogen desorption is the rate-determining step [27].

The nickel and cobalt in the form of carbon-supported cobalt catalysts can have a high ammonia conversion rate of about 350–400 °C due to weaker nitrogen binding and effectiveness activity [32]. The La-based perovskite, such as LaMO₃ (M = La-Co, La-Ni, La-Ce-Co and La-Ce-Ni) and LaCeNiO₃ catalyst, can replace Ru in the ammonia conversion due to their physical properties, the surface area and pore-size distribution. According to **Figure 14**,

ammonia decomposition over perovskite-type lanthanum-based catalysts increased at different temperatures in the range of 300–600 °C and at a GHSV of 6000 h⁻¹ [56].

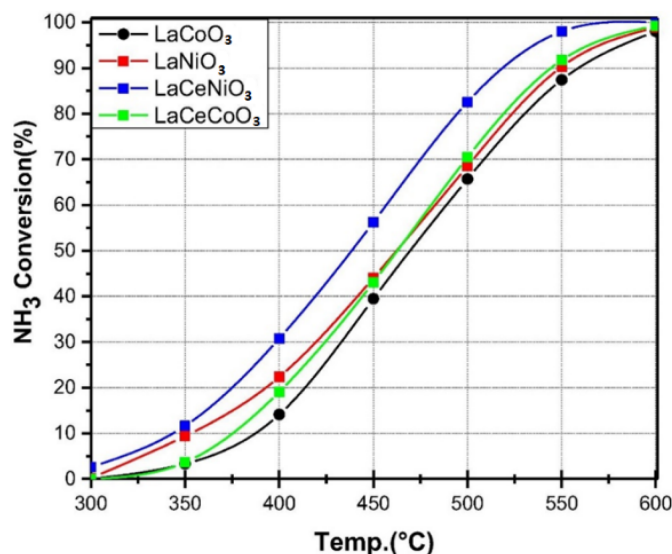


Figure 14. Comparison performance of lanthanum-based catalysts for ammonia decomposition. Reprinted with permission [56].

The ammonia decomposition reaction over perovskite-based polymers of a lanthanum-based catalyst consisting of calcined nickel and cobalt showed a higher catalytic performance for La- and Ni (LaNiO₃) than Co(LaCoO₃) catalyst, with a conversion rate of 99% at 450 °C (Figure 15) [57].

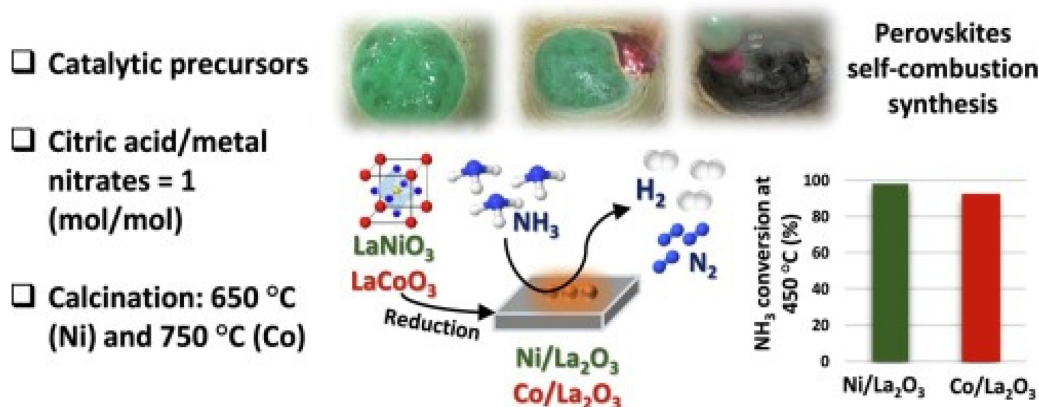


Figure 15. The process of ammonia decomposition over a La-based catalyst consists of calcined nickel and cobalt [57].

Nickel-based catalysts can be used for ammonia decomposition as highly efficient non-Ru catalysts. The catalytic performance of catalysts is significantly influenced by the properties of the support [58]. They need preparation procedures and are expensive. Their efficiency depends on supports, which are highly active if supported on ceramic materials and inactive on carbon materials [59]. Although, some of its components, such as the

$\text{Ni/MgAl}_2\text{O}_4$, can be used as an economical and highly efficient non-Ru catalyst. According to **Figure 16**, the $\text{Ni/MgAl}_2\text{O}_4$ -LDH catalyst with high thermal stability, through calcined layered double hydroxide (LDH) supports, showed an ammonia conversion efficiency rate of 90% at 600 °C [58].

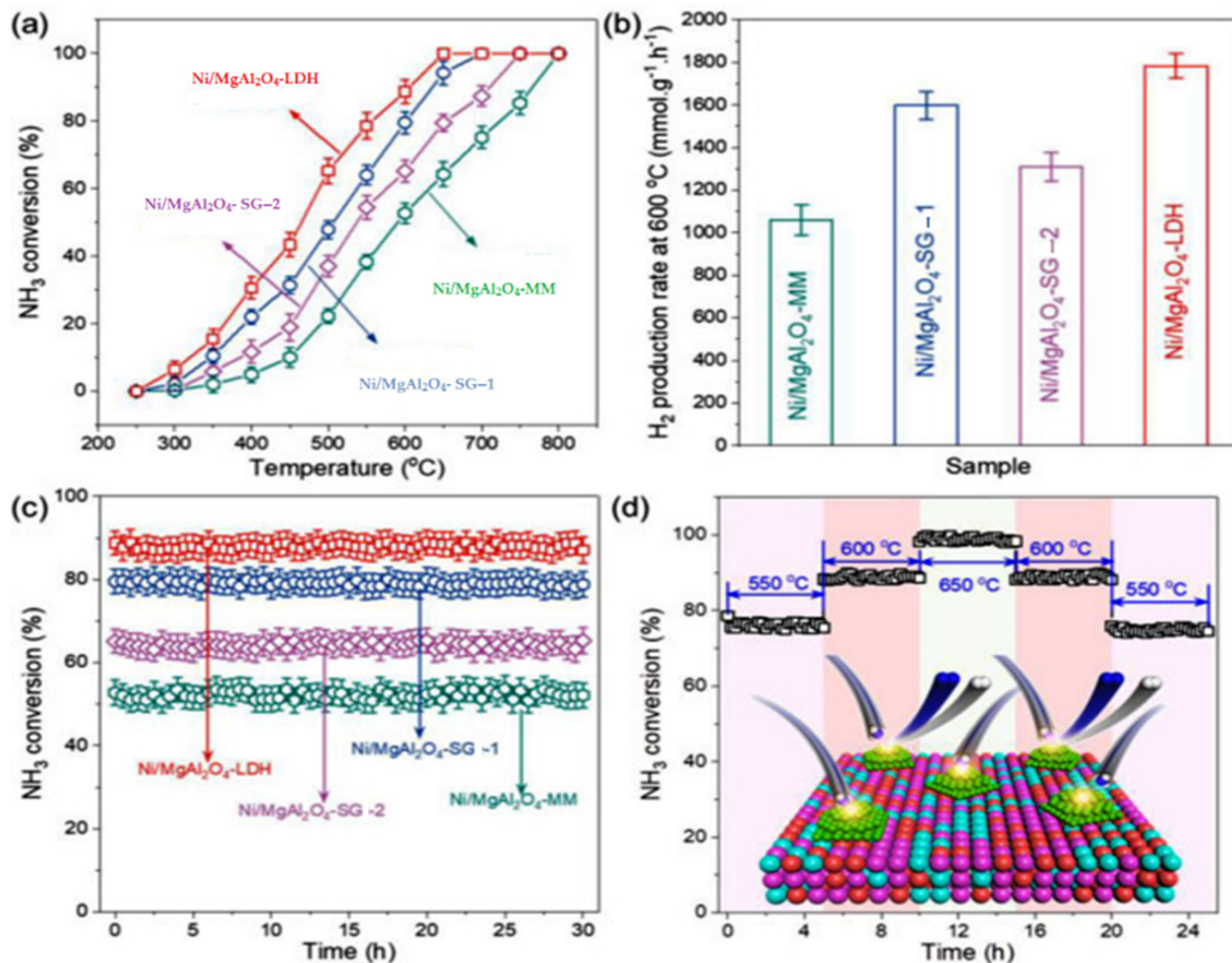


Figure 16. The effects of catalysts support properties on performance of ammonia decomposition at temperatures from 250 to 800 °C (a) ammonia conversion at different temperatures (b) different support catalysts with the highest conversion rate for the $\text{Ni/MgAl}_2\text{O}_4$ -LDH catalyst (c) time course of different support catalysts and (d) time course of ammonia conversion at 550 to 600 °C [58].

The main obstacle is hydrogen passivation/poisoning of the catalytic surface to attain a low-temperature conversion of the process. Furthermore, nitrogen association for this reaction can be rate-limited over an Mo_3N_2 cluster for an ammonia decomposition reaction. Some non-precious Mo_2N -based catalysts reached the highest decomposition of 100% at 823 K [33]. Furthermore, according to **Figure 17**, the ammonia decomposition over Ni-based catalysts on metal oxides supported with $\text{Ni/Y}_2\text{O}_3$ reached 99.74%, and the hydrogen formation rate was 47.88 mmol/min g_{cat} as a function of temperature [25][60].

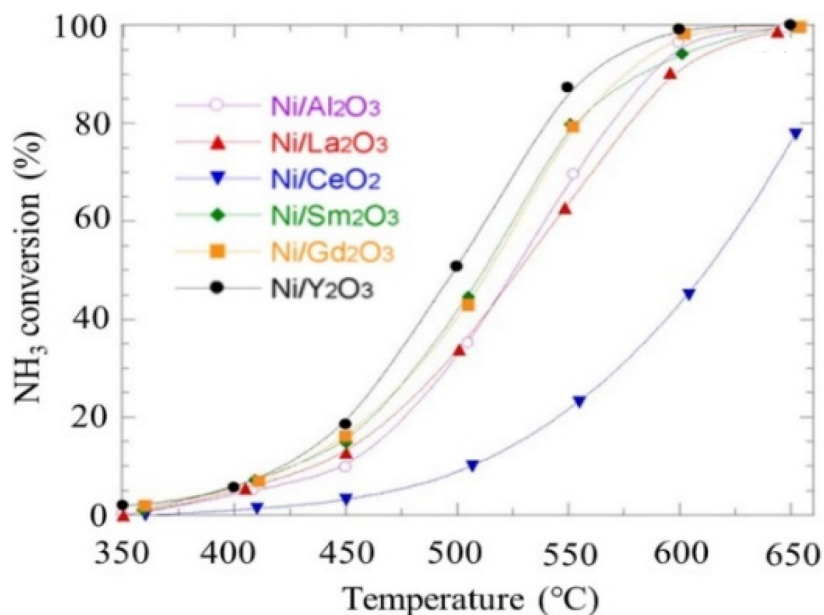


Figure 17. Ammonia cracking over Ni-based catalysts at different temperatures from 350 to 650 °C. the highest ammonia conversion rate at different temperatures reached with Ni/Y₂O₃. Reprinted with permission [25][60].

The sizes of nickel particles have an effect on their activity and their turnover frequencies (TOF) in the decomposition of ammonia. As displayed in **Figure 18**, the nickel particles with average sizes below 2.9 nm showed considerable activity, with an optimum value of 2.3 nm [43][61][62].

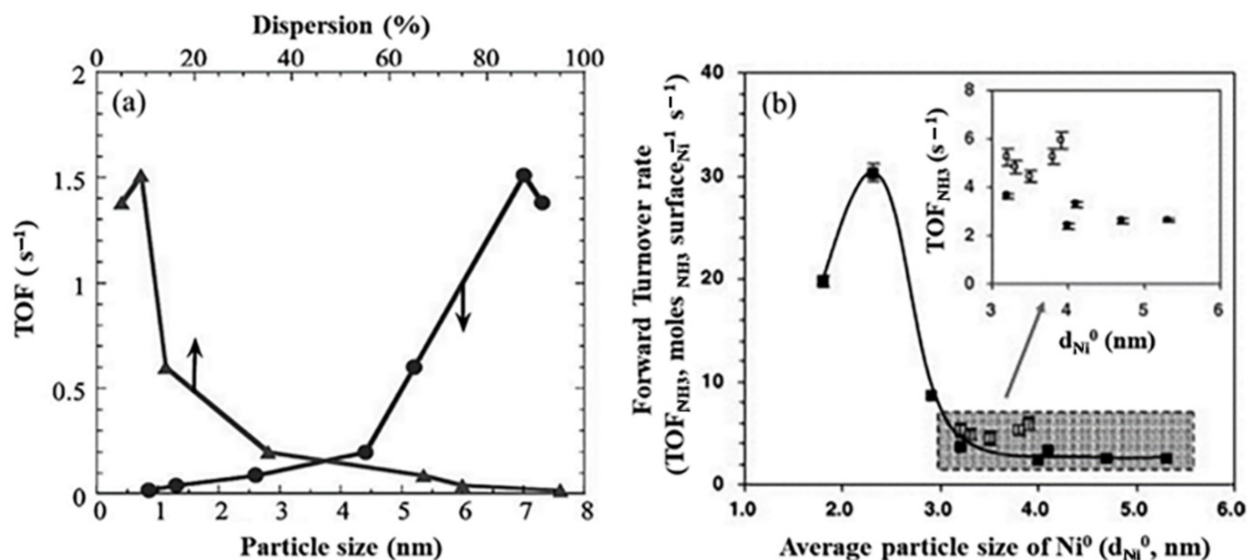


Figure 18. Relationship between the forward ammonia turnover rate (TOF) and average particle size (a) for Ni (circles) in compare with Ru (triangles), (b) for Ni–Al₂O₃ (solid squares) in compare with La–Al₂O₃ catalysts (hollow squares). Reprinted with permission [43][62][61].

The cobalt-based catalysts consisted of a promoter element of 1% K and the use of 5% Co. Silicon carbide support (β -SiC) showed an excellent conversion performance of 100% at 450 °C (**Figure 19**). The performance of cobalt was less than Ru, but it has a lower price and thus can be used as an alternative for developing a catalyst suitable for commercial purposes [59][63]. The Co_3O_4 nanoparticles were dispersed densely on the barium hexa-aluminate (BHA) surface, with excellent catalytic stability for high ammonia conversion rates [11].

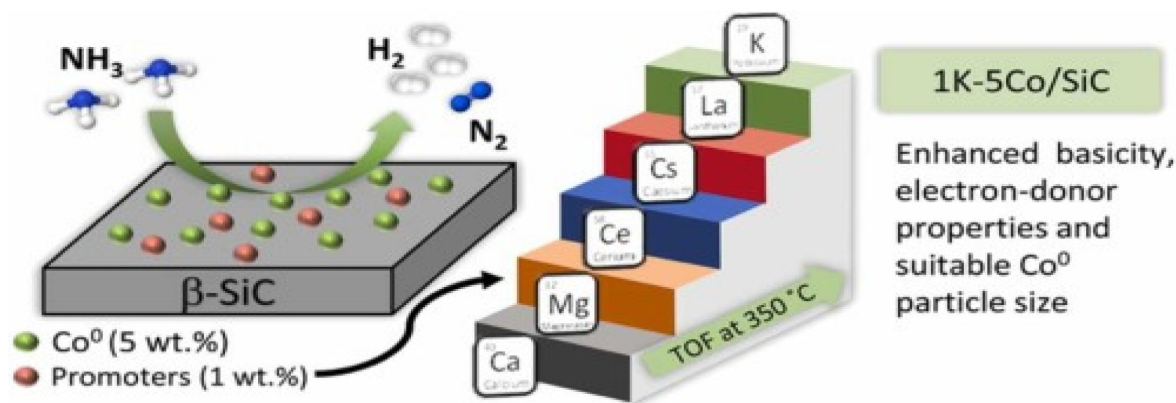
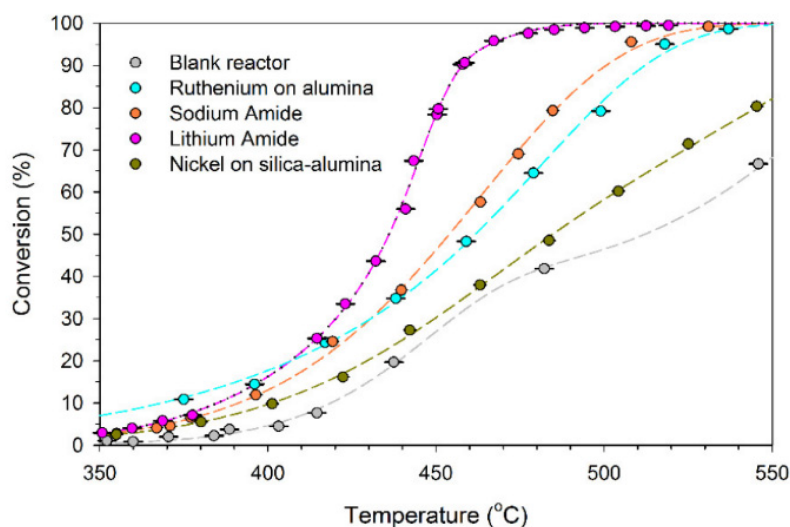


Figure 19. Cobalt-based catalysts, their support and promoters in ammonia decomposition. Reprinted with permission [59].

Using alkali metal imides and amides, such as sodium amide (NaNH_2) or lithium amide, Li_2NH , due to their unique reaction mechanism, can increase ammonia decomposition at temperatures lower than 450 °C compared with the higher temperatures above 600 °C required for other catalysts to reach 100% conversion efficiency [5]. A comparison of the performance of lithium and sodium amide supported with nickel (Ni) and ruthenium catalysts for ammonia decomposition into hydrogen is represented in **Figure 20** [64]. The catalytic performance of lithium for an ammonia flow rate of 500 sccm (cm^3/min) at 580–600 °C was 99% (for 1 g of lithium imide), which was higher than sodium and other catalysts [5][65].



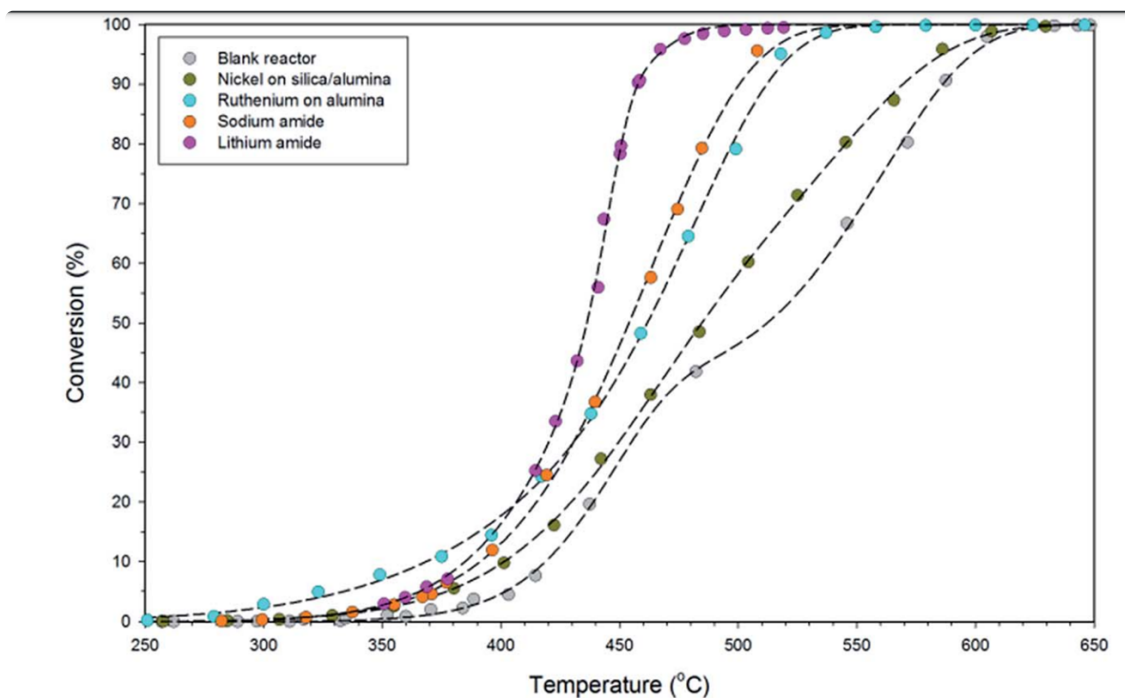


Figure 20. Comparison of catalytic activities of metal amides with supported nickel and ruthenium catalysts for ammonia conversion at 250–650 °C. Reprinted with permission^[66].

References

1. Dincer, I.; Acar, C. Review and evaluation of hydrogen production methods for better sustainability. *Int. J. Hydrogen Energy* 2015, 40, 11094–11111.
2. Ye, M.; Sharp, P.; Brandon, N.; Kucernak, A. System-level comparison of ammonia, compressed and liquid hydrogen as fuels for polymer electrolyte fuel cell powered shipping. *Int. J. Hydrogen Energy* 2022, 47, 8565–8584.
3. Cha, J.; Park, Y.; Brigljević, B.; Lee, B.; Lim, D.; Lee, T.; Jeong, H.; Kim, Y.; Sohn, H.; Mikulčić, H.; et al. An efficient process for sustainable and scalable hydrogen production from green ammonia. *Renew. Sustain. Energy Rev.* 2021, 152, 111562.
4. Kroposki, B.; Levene, J.; Harrison, K.; Sen, P.; Novachek, F. *Electrolysis: Information and Opportunities for Electric Power Utilities*; Technical Report NREL/TP-581-40605; NREL: Golden, CO, USA, 2006.
5. Mukherjee, S.; Devaguptapu, S.V.; Sviripa, A.; Lund, C.R.; Wu, G. Low-temperature ammonia decomposition catalysts for hydrogen generation. *Appl. Catal. B Environ.* 2018, 226, 162–181.
6. Li, G.; Kanezashi, M.; Yoshioka, T.; Tsuru, T. Ammonia decomposition in catalytic membrane reactors: Simulation and experimental studies. *AIChE J.* 2012, 59, 168–179.

7. Xie, T.; Xia, S.; Jin, Q. Thermodynamic Optimization of Ammonia Decomposition Solar Heat Absorption System Based on Membrane Reactor. *Membranes* 2022, 12, 627.
8. Do, S.-H.; Roh, J.S.; Park, H.B. Carbon-free Hydrogen Production Using Membrane Reactors. *Membr. J.* 2018, 28, 297–306.
9. Barisano, D.; Canneto, G.; Nanna, F.; Villone, A.; Fanelli, E.; Freda, C.; Grieco, M.; Lotierzo, A.; Cornacchia, G.; Braccio, G.; et al. Investigation of an Intensified Thermo-Chemical Experimental Set-Up for Hydrogen Production from Biomass: Gasification Process Integrated to a Portable Purification System—Part II. *Energies* 2022, 15, 4580.
10. Abashar, M.; Al-Sughair, Y.; Al-Mutaz, I. Investigation of low temperature decomposition of ammonia using spatially patterned catalytic membrane reactors. *Appl. Catal. A Gen.* 2002, 236, 35–53.
11. Li, G.; Yu, X.; Yin, F.; Lei, Z.; Zhang, H.; He, X. Production of hydrogen by ammonia decomposition over supported Co₃O₄ catalysts. *Catal. Today* 2022, 402, 45–51.
12. Chen, Y.-L.; Juang, C.-F.; Chen, Y.-C. The Effects of Promoter Cs Loading on the Hydrogen Production from Ammonia Decomposition Using Ru/C Catalyst in a Fixed-Bed Reactor. *Catalysts* 2021, 11, 321.
13. Cechetto, V.; Di Felice, L.; Medrano, J.A.; Makhoulfi, C.; Zuniga, J.; Gallucci, F. H₂ production via ammonia decomposition in a catalytic membrane reactor. *Fuel Process. Technol.* 2021, 216, 106772.
14. Abashar, M. Ultra-clean hydrogen production by ammonia decomposition. *J. King Saud Univ. Eng. Sci.* 2018, 30, 2–11.
15. Zhang, Z.; Liguori, S.; Fuerst, T.F.; Way, J.D.; Wolden, C.A. Efficient Ammonia Decomposition in a Catalytic Membrane Reactor To Enable Hydrogen Storage and Utilization. *ACS Sustain. Chem. Eng.* 2019, 7, 5975–5985.
16. Cechetto, V.; Di Felice, L.; Martinez, R.G.; Plazaola, A.A.; Gallucci, F. Ultra-pure hydrogen production via ammonia decomposition in a catalytic membrane reactor. *Int. J. Hydrogen Energy* 2022, 47, 21220–21230.
17. Heidenreich, S.; Müller, M.; Foscolo, P.U. Chapter 5—Advanced Process Combination Concepts. In *Advanced Biomass Gasification*; Heidenreich, S., Müller, M., Foscolo, P.U., Eds.; Academic Press: Cambridge, MA, USA, 2016; pp. 55–97.
18. Yang, X.; Wang, S.; He, Y. Review of catalytic reforming for hydrogen production in a membrane-assisted fluidized bed reactor. *Renew. Sustain. Energy Rev.* 2021, 154, 111832.
19. Lim, D.-K.; Plymill, A.B.; Paik, H.; Qian, X.; Zecevic, S.; Chisholm, C.R.; Haile, S.M. Solid Acid Electrochemical Cell for the Production of Hydrogen from Ammonia. *Joule* 2020, 4, 2338–2347.

20. Chiuta, S.; Everson, R.C.; Neomagus, H.W.; van der Gryp, P.; Bessarabov, D.G. Reactor technology options for distributed hydrogen generation via ammonia decomposition: A review. *Int. J. Hydrogen Energy* 2013, 38, 14968–14991.
21. Itoh, N.; Oshima, A.; Suga, E.; Sato, T. Kinetic enhancement of ammonia decomposition as a chemical hydrogen carrier in palladium membrane reactor. *Catal. Today* 2014, 236, 70–76.
22. Wang, W.; Padban, N.; Ye, Z.; Andersson, A.A.; Bjerle, I. Kinetics of Ammonia Decomposition in Hot Gas Cleaning. *Ind. Eng. Chem. Res.* 1999, 38, 4175–4182.
23. Demirbas, A. Future hydrogen economy and policy. *Energy Sources, Part B Econ. Planning, Policy* 2016, 12, 172–181.
24. Mazzone, S.; Campbell, A.; Zhang, G.; García-García, F. Ammonia cracking hollow fibre converter for on-board hydrogen production. *Int. J. Hydrogen Energy* 2021, 46, 37697–37704.
25. Wan, Z.; Tao, Y.; Shao, J.; Zhang, Y.; You, H. Ammonia as an effective hydrogen carrier and a clean fuel for solid oxide fuel cells. *Energy Convers. Manag.* 2020, 228, 113729.
26. Makepeace, J.W.; He, T.; Weidenthaler, C.; Jensen, T.R.; Chang, F.; Vegge, T.; Ngene, P.; Kojima, Y.; de Jongh, P.E.; Chen, P.; et al. Reversible ammonia-based and liquid organic hydrogen carriers for high-density hydrogen storage: Recent progress. *Int. J. Hydrogen Energy* 2019, 44, 7746–7767.
27. Lucentini, I.; Garcia, X.; Vendrell, X.; Llorca, J. Review of the Decomposition of Ammonia to Generate Hydrogen. *Ind. Eng. Chem. Res.* 2021, 60, 18560–18611.
28. Oni, A.; Anaya, K.; Giwa, T.; Di Lullo, G.; Kumar, A. Comparative assessment of blue hydrogen from steam methane reforming, autothermal reforming, and natural gas decomposition technologies for natural gas-producing regions. *Energy Convers. Manag.* 2022, 254, 115245.
29. Edwards, P.P.; Kuznetsov, V.L.; David, W.I.F. Hydrogen energy. *Philos. Trans. R. Soc. A Math. Phys. Eng. Sci.* 2007, 365, 1043–1056.
30. Dai Z, Ansaloni L, Deng L; Recent advances in multi-layer composite polymeric membranes for CO₂ separation: A review. *Green Energy & Environment* **2016** , 1;1(2), 102-28., 10.1016/j.gee.2016.08.001.
31. Dai Z, Ansaloni L, Deng L; Recent advances in multi-layer composite polymeric membranes for CO₂ separation: A review. *Green Energy & Environment* **2016** , 1;1(2), 102-28., 10.1016/j.gee.2016.08.001.
32. Seyfeli, R.C.; Varisli, D. Ammonia decomposition reaction to produce CO_x-free hydrogen using carbon supported cobalt catalysts in microwave heated reactor system. *Int. J. Hydrogen Energy* 2020, 45, 34867–34878.

33. Chen, C.; Wu, K.; Ren, H.; Zhou, C.; Luo, Y.; Lin, L.; Au, C.; Jiang, L. Ru-Based Catalysts for Ammonia Decomposition: A Mini-Review. *Energy Fuels* 2021, 35, 11693–11706.
34. Jung, S.-C.; Chung, K.-H.; Choi, J.; Park, Y.-K.; Kim, S.-J.; Kim, B.-J.; Lee, H. Photocatalytic hydrogen production using liquid phase plasma from ammonia water over metal ion-doped TiO₂ photocatalysts. *Catal. Today* 2022, 397–399, 165–172.
35. Obata, K.; Kishishita, K.; Okemoto, A.; Taniya, K.; Ichihashi, Y.; Nishiyama, S. Photocatalytic decomposition of NH₃ over TiO₂ catalysts doped with Fe. *Appl. Catal. B Environ.* 2014, 160–161, 200–203.
36. Yuzawa, H.; Mori, T.; Itoh, H.; Yoshida, H. Reaction Mechanism of Ammonia Decomposition to Nitrogen and Hydrogen over Metal Loaded Titanium Oxide Photocatalyst. *J. Phys. Chem. C* 2012, 116, 4126–4136.
37. Akkerman, Q.A.; Manna, L. What Defines a Halide Perovskite? *ACS Energy Lett.* 2020, 5, 604–610.
38. Assirey, E.A.R. Perovskite synthesis, properties and their related biochemical and industrial application. *Saudi Pharm. J.* 2019, 27, 817–829.
39. Hill, A.K.; Torrente-Murciano, L.T. Low temperature H₂ production from ammonia using ruthenium-based catalysts: Synergetic effect of promoter and support. *Appl. Catal. B Environ.* 2015, 172–173, 129–135.
40. Lamb, K.E.; Dolan, M.D.; Kennedy, D.F. Ammonia for hydrogen storage; A review of catalytic ammonia decomposition and hydrogen separation and purification. *Int. J. Hydrogen Energy* 2019, 44, 3580–3593.
41. Lente, G. Comment on “‘Turning Over’ Definitions in Catalytic Cycles”. *ACS Catal.* 2013, 3, 381–382.
42. Turnover Frequency—An Overview|ScienceDirect Topics. Available online: <https://www.sciencedirect.com/topics/chemistry/turnover-frequency> (accessed on 13 September 2022).
43. Bell, T.E.; Murciano, L.T. H₂ Production via Ammonia Decomposition Using Non-Noble Metal Catalysts: A Review. *Top. Catal.* 2016, 59, 1438–1457.
44. Chehade, G.; Dincer, I. Progress in green ammonia production as potential carbon-free fuel. *Fuel* 2021, 299, 120845.
45. Kozuch, S. and Martin, J.M.; Turning over definitions in catalytic cycles. *Acs Catalysis* **2012**, 2(12), 2787-2794.
46. Kozuch, S. and Martin, J.M.; Turning over definitions in catalytic cycles. *Acs Catalysis* **2012**, 2(12), 2787-2794.

47. Jiang, K.; Li, K.; Liu, Y.-Q.; Lin, S.; Wang, Z.; Wang, D.; Ye, Y. Nickel-cobalt nitride nanoneedle supported on nickel foam as an efficient electrocatalyst for hydrogen generation from ammonia electrolysis. *Electrochimica Acta* 2021, 403, 139700.
48. Jacobsen, C.J., Dahl, S., Clausen, B.S., Bahn, S., Logadottir, A.; Catalyst Design by Interpolation in the Periodic Table: Bimetallic Ammonia Synthesis Catalysts.. *J Am Chem Soc* **2001**, 123(34), 8404-8405..
49. Ganley, J.C., Thomas, F.S., Seebauer, E.G. and Masel, R.I.; A priori catalytic activity correlations: the difficult case of hydrogen production from ammonia. *Catal Letters*. **2004**, 96(3), 117-122..
50. Hansgen, D. A.; Vlachos, D. G.; Chen, J. G.; Using first principles to predict bimetallic catalysts for the ammonia decomposition reaction. *Nat Chem* **2010**, 2 (6), 484– 489, 10.1038/nchem.626 .
51. Mazzone, S.; Goklany, T.; Zhang, G.; Tan, J.; Papaioannou, E.I.; García-García, F. Ruthenium-based catalysts supported on carbon xerogels for hydrogen production via ammonia decomposition. *Appl. Catal. A Gen.* 2022, 632, 118484.
52. Yin, S.; Xu, B.; Zhu, W.; Ng, C.; Zhou, X.; Au, C. Carbon nanotubes-supported Ru catalyst for the generation of CO_x-free hydrogen from ammonia. *Catal. Today* 2004, 93–95, 27–38.
53. Yin, S.-F.; Xu, B.-Q.; Ng, C.-F.; Au, C.-T. Nano Ru/CNTs: A highly active and stable catalyst for the generation of CO_x-free hydrogen in ammonia decomposition. *Appl. Catal. B Environ.* 2004, 48, 237–241.
54. El-Shafie, M.; Kambara, S.; Hayakawa, Y. Development of zeolite-based catalyst for enhancement hydrogen production from ammonia decomposition. *Catal. Today* 2021, 397–399, 103–112.
55. Liu, Y.; Wang, H.; Yuan, X.; Wu, Y.; Wang, H.; Tan, Y.Z.; Chew, J.W. Roles of sulfur-edge sites, metal-edge sites, terrace sites, and defects in metal sulfides for photocatalysis. *Chem Catal.* 2021, 1, 44–68.
56. Podila, S.; Driss, H.; Ali, A.M.; Al-Zahrani, A.A.; Daous, M.A. Influence of Ce substitution in LaMO₃ (M = Co/Ni) perovskites for CO_x-free hydrogen production from ammonia decomposition. *Arab. J. Chem.* 2021, 15, 103547.
57. Pinzón, M.; Sánchez-Sánchez, A.; Sánchez, P.; de la Osa, A.; Romero, A. Ammonia as a carrier for hydrogen production by using lanthanum based perovskites. *Energy Convers. Manag.* 2021, 246, 114681.
58. Qiu, Y.; Fu, E.; Gong, F.; Xiao, R. Catalyst support effect on ammonia decomposition over Ni/MgAl₂O₄ towards hydrogen production. *Int. J. Hydrogen Energy* 2021, 47, 5044–5052.
59. Pinzón, M.; Romero, A.; de Lucas-Consuegra, A.; de la Osa, A.R.; Sánchez, P. CO_x-free hydrogen production from ammonia at low temperature using Co/SiC catalyst: Effect of promoter.

- Catalysis Today. *Int. J. Hydrogen Energy* 2022, 390, 34–47.
60. K. Okura, T. Okanishi, H. Muroyama, T. Matsui, K. Eguchi.; Ammonia Decomposition over Nickel Catalysts Supported on Rare-Earth Oxides for the On-Site Generation of Hydrogen. *Chem Cat Chem* **2016**, 8, 2988-2995.
 61. Zhang, J., Xu, H. and Li, W.; Kinetic study of NH₃ decomposition over Ni nanoparticles: The role of La promoter, structure sensitivity and compensation effect. . *Applied Catalysis A: General* **2005**, 296(2), 257-267.
 62. Karim, Ayman M., et al.; Correlating particle size and shape of supported Ru/ γ -Al₂O₃ catalysts with NH₃ decomposition activity. *J Am Chem Soc* **2009**, 131 (34), 12230-12239.
 63. Gholami, Z.; Tišler, Z.; Rubáš, V. Recent advances in Fischer-Tropsch synthesis using cobalt-based catalysts: A review on supports, promoters, and reactors. *Catal. Rev.* 2021, 63, 512–595.
 64. Makepeace, J.W., Wood, T.J., Hunter, H.M., Jones, M.O. and David, W.I.; Ammonia decomposition catalysis using non-stoichiometric lithium imide. *Chemical science* **2015**, 6(7), 3805-3815.
 65. Jackson, C.; Fothergill, K.; Gray, P.; Haroon, F.; Makhloufi, C.; Kezibri, N.; Davey, A.; Hote, O.L.; Zarea, M.; Davenne, T.; et al. Ammonia to Green Hydrogen Project; Feasibility Study; Ecuity: Birmingham, UK, 2020; pp. 1–70.
 66. Makepeace, J.W., Wood, T.J., Hunter, H.M., Jones, M.O. and David, W.I.; Ammonia decomposition catalysis using non-stoichiometric lithium imide. *Chemical science* **2015**, 6(7), 3805-3815.

Retrieved from <https://encyclopedia.pub/entry/history/show/86393>